

Article

Force Dependent Quantum Phase Transition in the Hybrid Optomechanical System

Lingchao Li ¹ and Jian-Qi Zhang ^{2,*} ¹ College of Science, Henan University of Technology, Zhengzhou 450001, China; aoneer@163.com² State Key Laboratory of Magnetic Resonance and Atomic and Molecular Physics, Wuhan Institute of Physics and Mathematics, Innovation Academy of Precision Measurement Science and Technology, Chinese Academy of Sciences, Wuhan 430071, China

* Correspondence: changjianqi@gmail.com

Abstract: The optomechanics shows a great potential in quantum control and precise measurement due to appropriate mechanical control. Here we theoretically study the quantum phase transition in a hybrid atom-optomechanical cavity with an external force. Our study shows, in the thermodynamic limit, the critical value of quantum phase transition between the normal phase and super-radiant phase can be controlled and modified by the external force via the tunable frequency of optomechanics, then a force dependent quantum phase transition can be achieved in our system. Moreover, this force dependent quantum phase transition can be employed to detect the external force variation. In addition, our numerical simulations illustrate the sensitivity of the external force measurement can be improved by the squeezing properties of the quantum phase transition.

Keywords: quantum phase transition; external force measurement; squeezing; optomechanics

PACS: 05.70.Fh; 03.65.Ta; 42.50.Lc; 42.50.Wk



Citation: Li, L.; Zhang, J.-Q. Force Dependent Quantum Phase Transition in the Hybrid Optomechanical System. *Photonics* **2021**, *8*, 588. <https://doi.org/10.3390/photonics8120588>

Received: 28 October 2021
Accepted: 12 December 2021
Published: 18 December 2021

Publisher's Note: MDPI stays neutral with regard to jurisdictional claims in published maps and institutional affiliations.



Copyright: © 2021 by the authors. Licensee MDPI, Basel, Switzerland. This article is an open access article distributed under the terms and conditions of the Creative Commons Attribution (CC BY) license (<https://creativecommons.org/licenses/by/4.0/>).

1. Introduction

Optomechanical cavity works as an ideal platform to study the quantum properties of macroscopic mechanical systems. It has attracted great attentions to explore many interesting quantum properties, such as squeezing and entanglement [1–5], optomechanically induced transparency [6–10] and chaos [11,12], which are associated with potential applications in quantum information processing [13,14], ground state cooling of the mechanical modes [15–22] and precision measurement [10,23,24].

On the other hand, the Dicke model, constituted of an atomic ensemble and a single-mode cavity, is one of essential model describing the collective effects in quantum optics [25,26]. With the increase of the atom-cavity coupling, the Dicke model undergoes a quantum phase transition (QPT) from the normal phase to the super-radiant one [27,28]. The QPT is first predicted at weak coupling in the thermodynamic limit [29], and then it is used to explore chaotic signatures [30–34], entanglement properties of the single mode of super-radiance [35], and scaled physical quantities [36,37]. Simultaneously, a theoretical proposal predicts it is possible to get an effective Dicke model with multilevel atoms and cavity-mediated Raman transitions [38], and this effective Dicke model has been observed in the superconducting qubits system [39].

Recently, there exists a growing interest in the QPT of hybrid atom-optomechanical system [40–50], which are motivated by the need to understand the interplay between QPT and optomechanical properties [51–53] as well as by the applications of precision measurements [54,55]. However, limited by the certain frequencies of qubit and cavity mode, it remains a challenge to construct the QPT taking the critical value with a feature of tunability.

In this scheme, we illustrate it is possible to control the critical value of QPT in a hybrid atom-optomechanical system via an external force. The critical value of the QPT between the normal phase and the super-radiant phase can be shifted by adjusting the external force, which can modify the frequency of the optomechanical cavity via its effective length. Therefore, there exists a force dependent QPT in our hybrid atom-optomechanical system. Moreover, this force dependent QPT can also be applied to precisely detect the external force via the critical value of the QPT. In addition, our numerical calculations show there would be slight squeezing of the quadrature variances of atoms and cavity field in the thermodynamic limit. Specially, the squeezing degree of cavity field can be enhanced by increasing the external force, and the best squeezing degree occurs around the critical value of QPT, which can be selected by the external force.

Compared to the previous works for QPT, our scheme takes some significant differences. First of all, our study shows the critical value of the QPT can be controlled by the external force, which can be employed to realize a force dependent QPT. Therefore, our proposal overcomes the limitation of the critical value of the QPT without tunability [51–54] by introducing an external force. Secondly, our work focuses on the tunability of critical value of the QPT from normal phase to super-radiant phase without dissipations, and squeezing properties are considered to realize the precision measurement. By contrast, tunable critical atom-photon coupling strength in the previous work [56] is for a bifurcation point resulting from dissipations, and no squeezing properties is involved in precision measurement. Finally, our precise measurement is based on squeezing properties of QPT rather than the input squeezed field. Without the driven field, the squeezing properties in super-radiant phase not only ensures the force measurement in the hybrid atom-optomechanical system is out of reach for the traditional optomechanics without squeezing properties [10,23,24], but also paves a way to enhance the sensitivity with the squeezing properties of QPT.

2. Model and Hamiltonian

As it is depicted in Figure 1, the whole Hamiltonian can be written as a sum of two parts as

$$H = H_D + H_m. \tag{1}$$

The first part H_D is the Hamiltonian of Dicke model, where an ensemble of N two-level atoms taking a transition frequency ω_0 is trapped in a single-mode cavity at frequency ω_a . It can be presented as

$$H_D = \hbar\omega_a a^\dagger a + \hbar\omega_0 J_z + \frac{\hbar\chi}{\sqrt{N}}(a^\dagger + a)(J_+ + J_-), \tag{2}$$

where the first two items are the free Hamiltonians of the single-mode cavity field and atomic ensemble. a^\dagger and a denote creation and annihilation operators of the single-mode cavity field, respectively. The last term shows the interaction between the atomic ensemble and cavity mode with a coupling strength χ . J_+ , J_- , and J_z are the collective atomic operators following the commutation relations as $[J_+, J_-] = 2J_z$ and $[J_z, J_\pm] = \pm J_\pm$. χ is the coupling strength between the atomic ensemble and the cavity field.

The second part H_m is the Hamiltonian of optomechanical cavity [57], where the cavity mode couples to the mechanical mode with frequency ω_m and mass m via a radiation pressure interaction. The mechanical mode is forced by an external force f . It can be described by

$$H_m = \frac{P_m^2}{2m} + \frac{1}{2}m\omega_m^2 Q_m^2 - \hbar g_0 a^\dagger a Q_m + f Q_m. \tag{3}$$

where Q_m and P_m are position and momentum operators of the mechanical mode, respectively. The first two items are the free energy of the mechanical mode, the third item describes the radiation pressure coupling taking a strength g_0 , and the last item shows the mechanical mode is driven by an external force f .

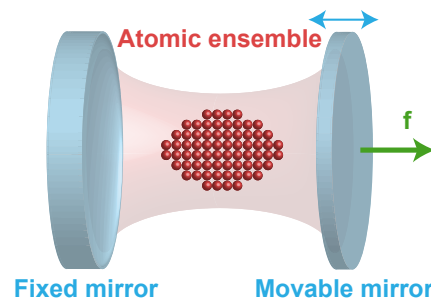


Figure 1. The hybrid atom-optomechanical cavity with an external force. Here an ensemble of N two-level atoms is trapped in the cavity optomechanics, the left cavity mirror is fixed and the right mirror can be moved, and the movable mirror is driven by an external force f .

Define $\tilde{Q}_m = Q_m + \frac{f}{m\omega_m^2} = (c + c^\dagger)/\sqrt{2m\omega_m}$ and $P_m = i(c^\dagger - c)/\sqrt{2m\omega_m}$, the Hamiltonian (1) can be rewritten as [54]

$$H = \tilde{\omega}_a a^\dagger a + \omega_m c^\dagger c + \omega_0 J_z - \frac{g}{N} a^\dagger a (c^\dagger + c) + \frac{\chi}{\sqrt{N}} (a^\dagger + a) (J_+ + J_-), \quad (4)$$

where the effective radiation pressure coupling is $g = Ng_0/\sqrt{2m\omega_m}$, and the effective frequency of optomechanical cavity

$$\tilde{\omega}_a = \omega_a + \frac{fg_0}{m\omega_m^2}, \quad (5)$$

is linear to the external force f . Note that the constant items have been ignored from Hamiltonian (4).

3. Normal Phase and Super-Radiant Phase

As the critical value for Dicke Hamiltonian is determined by the frequencies of single mode cavity field and atomic ensemble [58], the tunable effective frequency of the optomechanical cavity (5) reminds us that it is possible to modify the critical value with the external force, and achieve a force dependent QPT between normal phase and super-radiant phase. To illustrate this force dependent QPT in theory, we need to derive the equations about QPT as follows.

With the employment of the Holstein-Primakoff transformation, we can define

$$\begin{cases} J_+ &= b^\dagger \sqrt{N - b^\dagger b}, \\ J_- &= \sqrt{N - b^\dagger b} b, \\ J_z &= b^\dagger b - \frac{N}{2}, \end{cases} \quad (6)$$

where b^\dagger and b are bosonic operators satisfying the communication relation $[b, b^\dagger] = 1$.

Then, the Hamiltonian (4) can be rewritten as

$$H = \tilde{\omega}_a a^\dagger a + \omega_m c^\dagger c + \omega_0 b^\dagger b - \frac{g}{N} a^\dagger a (c^\dagger + c) + \chi (a^\dagger + a) (b^\dagger \sqrt{1 - \frac{b^\dagger b}{N}} + \sqrt{1 - \frac{b^\dagger b}{N}} b), \quad (7)$$

its parity operator can be given as

$$\Xi = \exp\{i[a^\dagger a + b^\dagger b + c^\dagger c]\}. \quad (8)$$

According to the method in Ref. [58], we can describe the QPT between the normal phase and super-radiant phase with two different mathematical methods.

3.1. Normal Phase

To calculate the eigenenergy of the normal phase, we assume the system works in the thermodynamic limit, where the number of atoms approaches an infinite value ($N \rightarrow \infty$). In this situation, both the numbers of excited atoms and photons are too small to be ignored ($\lim_{N \rightarrow \infty} \sqrt{1 - \frac{b^\dagger b}{N}} = 1$ and $\lim_{N \rightarrow \infty} \frac{a^\dagger a}{N} = 0$). Then the Hamiltonian (7) can be reduced to the normal phase Hamiltonian as

$$H^{NP} = \omega_m c^\dagger c + \tilde{\omega}_a a^\dagger a + \omega_0 b^\dagger b + \chi(a^\dagger + a)(b^\dagger + b), \tag{9}$$

after the constant item is ignored. The above Hamiltonian shows the mechanical mode is almost decoupled from the single-mode cavity field, while there is a bilinear coupling between the atomic ensemble and cavity mode. Therefore, the above normal phase Hamiltonian (9) can be diagonalized in the following.

Define the position and momentum operators of the two bosonic modes (a and b) as

$$\begin{cases} q_a = \frac{1}{\sqrt{2\tilde{\omega}_a}}(a^\dagger + a) & , & p_a = i\sqrt{\frac{\tilde{\omega}_a}{2}}(a^\dagger - a), \\ q_b = \frac{1}{\sqrt{2\omega_0}}(b^\dagger + b) & , & p_b = i\sqrt{\frac{\omega_0}{2}}(b^\dagger - b), \end{cases} \tag{10}$$

the Hamiltonian (9) can be rewritten as

$$H^{NP} = \omega_m c^\dagger c + \frac{1}{2}(\tilde{\omega}_a^2 q_a^2 + p_a^2 - \omega_0) + \frac{1}{2}(\omega_0^2 q_b^2 + p_b^2 - \tilde{\omega}_a) + 4\chi\sqrt{\tilde{\omega}_a\omega_0}q_a q_b, \tag{11}$$

which can be diagonalized with the collective coordinate operators as

$$\begin{cases} q_a = x_1 \cos \theta_1 + x_2 \sin \theta_1, \\ q_b = -x_1 \sin \theta_1 + x_2 \cos \theta_1. \end{cases} \tag{12}$$

with the angle θ_1 satisfying

$$\tan(2\theta_1) = \frac{4\chi\sqrt{\tilde{\omega}_a\omega_0}}{\omega_0^2 - \tilde{\omega}_a^2}. \tag{13}$$

When the atomic ensemble is in resonance with the effective frequency of cavity mode ($\tilde{\omega}_a = \omega_0$ and $\theta_1 = \frac{\pi}{4}$), the coordinate operators can be written as $q_a = (x_1 + x_2)/\sqrt{2}$ and $q_b = (-x_1 + x_2)/\sqrt{2}$, and the interaction term $q_a q_b$ in the Hamiltonian (11) can be eliminated. Then, the normal phase Hamiltonian (9) can be rewritten as

$$H^{NP} = \omega_m c^\dagger c + \frac{1}{2}[(\lambda_-^N)^2 x_1^2 + y_1^2 - \omega_0] + \frac{1}{2}[(\lambda_+^N)^2 x_2^2 + y_2^2 - \tilde{\omega}_a], \tag{14}$$

where λ_\pm^N are the energies of two hybrid bosonic modes for the atomic ensemble and cavity mode.

With the employment of definitions as

$$\begin{cases} x_1 = \frac{1}{\sqrt{2\lambda_-^N}}(d_1^\dagger + d_1) & , & y_1 = i\sqrt{\frac{\lambda_-^N}{2}}(d_1^\dagger - d_1), \\ x_2 = \frac{1}{\sqrt{2\lambda_+^N}}(d_2^\dagger + d_2) & , & y_2 = i\sqrt{\frac{\lambda_+^N}{2}}(d_2^\dagger - d_2), \end{cases} \tag{15}$$

the Hamiltonian (14) can be expressed with three decoupled bosonic modes as

$$H^{NP} = \omega_m c^\dagger c + \lambda_-^N d_1^\dagger d_1 + \lambda_+^N d_2^\dagger d_2 + \frac{1}{2}(\lambda_+^N + \lambda_-^N - \omega_0 - \tilde{\omega}_a). \tag{16}$$

Here the bosonic operators $\{d_1^\dagger, d_1, d_2^\dagger, d_2\}$ are the linear combinations of the original operators $\{a^\dagger, a, b^\dagger, b\}$ (see Appendix A). The energies of two bosonic modes λ_{\pm}^N can be presented as

$$(\lambda_{\pm}^N)^2 = \frac{1}{2} \{ \tilde{\omega}_a^2 + \omega_0^2 \pm \sqrt{(\omega_0^2 - \tilde{\omega}_a^2)^2 + 16\chi^2 \tilde{\omega}_a \omega_0} \}. \tag{17}$$

Specially, to ensure the excited energy λ_{-}^N is real, it is necessary to satisfy

$$\sqrt{(\omega_0^2 - \tilde{\omega}_a^2)^2 + 16\chi^2 \tilde{\omega}_a \omega_0} \leq \tilde{\omega}_a^2 + \omega_0^2, \tag{18}$$

which is corresponding to $\chi \leq \sqrt{\tilde{\omega}_a \omega_0} / 2 = \chi_c$. Here the atom-field coupling strength χ_c is the critical value of QPT between the normal phase and super-radiant phase. For this reason, the normal phase Hamiltonian H^{NP} remains valid when the coupling strength is not larger than the critical value ($\chi \leq \chi_c$). Noted that Hamiltonian H^{NP} commutes with the parity operator Ξ , and thus the eigenstates of H^{NP} have a definite parity in the normal phase.

3.2. Super-Radiant Phase

On the other hand, with the increase of the coupling strength χ , when this coupling strength is large enough, the system will take a QPT from the normal phase ($\chi < \chi_c$) to the super-radiant phase ($\chi > \chi_c$). In the super-radiant phase, both the atomic ensemble and the single mode cavity field acquire macroscopic occupations.

Define displacements of the bosonic modes as [58]:

$$a^\dagger \rightarrow A^\dagger + \sqrt{\alpha} \quad (\alpha \neq 0), \quad b^\dagger \rightarrow B^\dagger - \sqrt{\beta} \quad (\beta \neq 0), \tag{19}$$

with the assistance of displacement transformation of Equation (19), the Hamiltonian (7) can be rewritten as

$$\begin{aligned} H = & \tilde{\omega}_a(A^\dagger + \sqrt{\alpha})(A + \sqrt{\alpha}) + \omega_m c^\dagger c + \omega_0(B^\dagger - \sqrt{\beta})(B - \sqrt{\beta}) \\ & + \chi(A^\dagger + A + 2\sqrt{\alpha})(B^\dagger \sqrt{\xi} + \sqrt{\xi} B - 2\sqrt{\xi} \sqrt{\beta}) \\ & - \frac{g}{N}(A^\dagger + \sqrt{\alpha})(A + \sqrt{\alpha})(c^\dagger + c), \end{aligned} \tag{20}$$

with

$$\sqrt{\xi} = \sqrt{1 - \frac{(B^\dagger - \sqrt{\beta})(B - \sqrt{\beta})}{N}}.$$

Setting the terms with overall powers of N in the denominator to zero, and defining

$$\sqrt{\alpha} = \frac{\chi}{\tilde{\omega}_a} \sqrt{N(1 - \mu^2)}, \quad \sqrt{\beta} = \sqrt{\frac{N}{2}(1 - \mu)}, \quad \mu = \frac{\tilde{\omega}_a \omega_0}{4\chi^2} = \frac{\chi_c^2}{\chi^2}, \tag{21}$$

we can rewrite the Hamiltonian (20) in a bilinear form as [54]

$$H^{SP} = H_D^{SP} + \omega_m c^\dagger c - \Omega(c^\dagger + c), \tag{22}$$

where

$$\begin{aligned} H_D^{SP} = & \tilde{\omega}_a A^\dagger A + \tilde{\omega}_0 B^\dagger B + \frac{\omega_0(1-\mu)(3+\mu)}{8\mu(1+\mu)}(B^\dagger + B)^2 \\ & + \chi\mu \sqrt{\frac{2}{1+\mu}}(A^\dagger + A)(B^\dagger + B), \end{aligned} \tag{23}$$

$\tilde{\omega}_0 = \frac{\omega_0}{2\mu}(1 + \mu)$ and $\Omega = \frac{g\chi^2(1-\mu^2)}{\tilde{\omega}_a^2}$. The Hamiltonian (22) shows, in the super-radiant phase, although the moving mirror effectively decouples from the Dicke Hamiltonian part (23), it still suffers an effective classical driving force for the macroscopically excited field and atoms. Moreover, as the critical value χ_c of QPT depends on the effective frequency $\tilde{\omega}_a$, which is linear to the external force for Equation (5), it is possible to control this super-radiant phase with the external force.

To diagonalize the bilinear Hamiltonian (23), we move H^{SP} into the position-momentum representation with the following definitions

$$\begin{cases} X_a = \frac{1}{\sqrt{2\tilde{\omega}_a}}(A^\dagger + A) & , & P_a = i\sqrt{\frac{\tilde{\omega}_a}{2}}(A^\dagger - A), \\ X_b = \frac{1}{\sqrt{2\tilde{\omega}_0}}(B^\dagger + B) & , & P_b = i\sqrt{\frac{\tilde{\omega}_0}{2}}(B^\dagger - B), \\ X_c = \frac{1}{\sqrt{2\omega_m}}(c^\dagger + c) & , & P_c = i\sqrt{\frac{\omega_m}{2}}(c^\dagger - c), \end{cases} \quad (24)$$

and assumptions

$$\begin{cases} X_a = Q_1 \cos \theta_2 + Q_2 \sin \theta_2, \\ X_b = -Q_1 \sin \theta_2 + Q_2 \cos \theta_2, \end{cases} \quad (25)$$

here the angle θ_2 follows

$$\tan(2\theta_2) = \frac{2\tilde{\omega}_a\omega_0\mu^2}{\omega_0^2 - \mu^2\tilde{\omega}_a^2}.$$

Then the Hamiltonian (23) can be reduced to

$$H^{SP} = \frac{1}{2}\{(\lambda_-^S)^2 Q_1^2 + P_1^2 + (\lambda_+^S)^2 Q_2^2 + P_2^2 - \tilde{\omega}_0 - \tilde{\omega}_a\} + \frac{1}{2}(\omega_m^2 \tilde{X}_c^2 + P_c^2) - \frac{\Omega^2}{2\omega_m^2}, \quad (26)$$

with $\tilde{X}_c = X_c - \frac{\Omega}{\omega_m^2}$.

After three new bosonic modes $e_{1,2,3}$ as Equation (15) is introduced, the above Hamiltonian be rewritten as

$$H^{SP} = \lambda_-^S e_1^\dagger e_1 + \lambda_+^S e_2^\dagger e_2 + \lambda_0^S e_3^\dagger e_3 + \frac{1}{2}\{\lambda_-^S + \lambda_+^S - \tilde{\omega}_0 - \tilde{\omega}_a - \frac{\Omega^2}{\omega_m^2}\}, \quad (27)$$

where energies of three bosonic modes are

$$\begin{cases} (\lambda_\pm^S)^2 = \frac{1}{2}\{\tilde{\omega}_a^2 + \frac{\omega_0^2}{\mu^2} \pm \sqrt{(\frac{\omega_0^2}{\mu^2} - \tilde{\omega}_a^2)^2 + 4\tilde{\omega}_a^2\omega_0^2}\}, \\ \lambda_0^S = \omega_m, \end{cases} \quad (28)$$

new bosonic modes $e_{1,2}$ can be in terms of the original operators $\{A^\dagger, A, B^\dagger, B\}$ as Appendix A, and e_3 is the mechanical mode with a shifted steady position, which is caused by the excited cavity mode in the super-radiant phase via the radiation pressure interaction.

Specially, when $\tilde{\omega}_a^2 + \frac{\omega_0^2}{\mu^2} \geq \sqrt{(\frac{\omega_0^2}{\mu^2} - \tilde{\omega}_a^2)^2 + 4\tilde{\omega}_a^2\omega_0^2}$, or equivalently, $\chi \geq \sqrt{\tilde{\omega}_a\omega_0}/2 = \chi_c$, the excitation energy λ_-^S in Equation (27) can be kept in real. Hence, the Hamiltonian H^{SP} (27) can only be employed to describe the system in the super-radiant phase ($\chi \geq \chi_c$).

In this situation, the global symmetry Ξ would be broken at the QPT, while two new local symmetries for traditional super-radiant phase [58] still be achieved. These local symmetries are corresponding to the parity operator

$$\Xi^{SP} = \exp\{i\pi[A^\dagger A + B^\dagger B + c^\dagger c]\},$$

for the mean-field displacements. This operator would commute with the appropriate super-radiant Hamiltonian ($[\Xi^{SP}, H^{SP}] = 0$). Moreover, although the external force cannot change the symmetry of the system, the critical value of the QPT can be shifted by the external force.

4. Simulations and Discussion

In this section, we would like to give some simulations to demonstrate the force dependent quantum phase transition, and its applications on the external force measurement taking squeezing properties.

4.1. Force Dependent Quantum Phase Transition

The above two effective Hamiltonians describe the hybrid atom-optomechanical system versus the atom-cavity coupling χ in the thermodynamic limit ($N \rightarrow \infty$). Now, we would like to illustrate physical properties of these two effective Hamiltonians in different phases and show how to control the QPT via the external force. As the energy of mechanical mode ($\lambda_0 = \omega_m$) is very trivial, we don't present its calculations in the following.

When there is no external force ($f = 0$), as it is plotted in Figure 2, fundamental excitations energies of the system λ_{\pm} are the functions of coupling strength χ . According to the nature of the excitation for $\chi = 0$, the energies λ_- (black solid curve) and λ_+ (red dashed curve) can be named as photonic and atomic branches, respectively. Moreover, Figure 2 also shows, when the coupling strength approaches the critical value χ_c for QPT, the excitation energy of the photonic mode will vanish ($\lambda_- \rightarrow 0$), which implies the existence of the QPT. On the contrary, the trend of λ_+ approaches to the value $\sqrt{\omega_a^2 + \omega_0^2}$ when $\chi \rightarrow \chi_c$. In addition, in the asymptotic limit of $\chi \rightarrow \infty$, we can find $\lambda_- \rightarrow \omega_a$ as Equation (28), which means the energy will return to its initial value at $\chi = 0$, whereas $\lambda_+ \rightarrow 4\chi^2/\omega_a$. The critical exponents for this QPT are manifested in the behavior of the excitation energies [59].

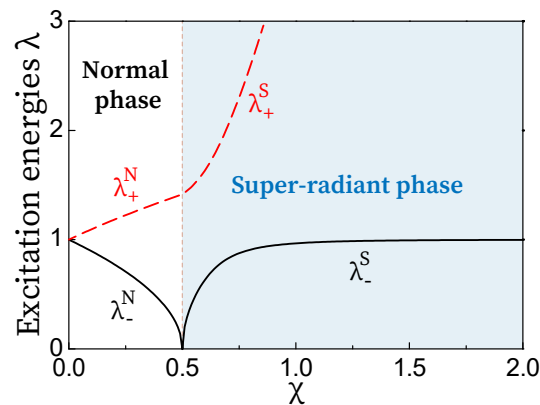


Figure 2. The excitation energies of the hybrid optomechanical system $\lambda = \lambda_{\pm}^{N,S}$ is plotted as the coupling strength χ for no external force ($f = 0$) by using Equations (17) and (28). The behavior of energy λ_- can be seen as “photonic” branch, denoted by black line and that of energy λ_+ can be seen as “atomic” branch, denoted by red line. Here we assume $\omega_0 = \omega_a = 1$, and then the value of λ_- vanishes at critical value $\chi = \chi_c = 0.5$, which denotes the occurrence of the QPT.

Next, we will show there exists the force dependent QPT in our system. Figure 3a presents the critical value of QPT for the different external force. It results from the fact that the external force works as the function of the critical value of QPT for

$$\chi_c = \sqrt{\tilde{\omega}_a \omega_0} / 2 = \sqrt{(\omega_a + \frac{f g_0}{m \omega_m^2}) \omega_0} / 2. \tag{29}$$

The external force f can be rewritten as a force ratio $\eta = f / f_0 = 4\chi_c^2 / (\omega_a \omega_0) - 1$ with $f_0 = m \omega_a \omega_m^2 / g_0$, then the force dependent frequency of the optomechanical cavity (5) can be rewritten as

$$\tilde{\omega}_a = \omega_a + \frac{f g_0}{m \omega_m^2} = \omega_a (1 + f / f_0) = \omega_a (1 + \eta). \tag{30}$$

Therefore, the critical value of the QPT can be modified by the external force. To illustrate this point for further, the force ratio η versus the critical value of QPT χ_c is plotted in Figure 3b. It presents that each critical values of QPT corresponds to one external force, which is linear to the force ratio ($f \propto \eta = f / f_0$). In detail, when $f > 0$, the external force will increase the frequency of optomechanics cavity, otherwise, the external force will

decrease the frequency of optomechanics cavity. As a result, there is a force dependent QPT in our system.

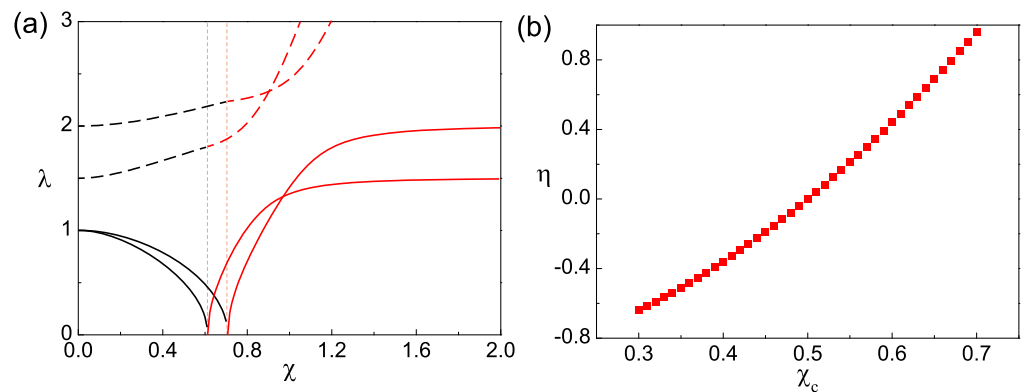


Figure 3. (a) The excitation energies of the hybrid atom–optomechanical system $\lambda = \lambda_{\pm}^{N,S}$ are plotted as functions of coupling strength χ by using Equations (17) and (28). The left (right) QPT is for the external force $f = 0.5f_0$ ($f = f_0$) with $f_0 = m\omega_a\omega_m^2/g_0$. (b) The force ratio $\eta = f/f_0$ is plotted as the function of the critical value of QPT χ_c with Equations (29) and (30). The other parameters are same as Figure 2.

4.2. Force Measurement Based on Squeezed Field

Now, we would like to illustrate the squeezing properties of our system and their application in the force measurement.

When the system is only microscopically excited, two quadrature variances of the cavity mode a can be defined by $(\Delta q_a)^2 = \langle q_a^2 \rangle - \langle q_a \rangle^2$ and $(\Delta p_a)^2 = \langle p_a^2 \rangle - \langle p_a \rangle^2$, which take the forms as

$$\begin{cases} (\Delta q_a)^2 &= \frac{1}{2\tilde{\omega}_a} \{1 + \langle a^{\dagger 2} \rangle + \langle a^2 \rangle + 2\langle a^\dagger a \rangle - (\langle a^\dagger \rangle + \langle a \rangle)^2\}, \\ (\Delta p_a)^2 &= \frac{\tilde{\omega}_a}{2} \{1 - \langle a^{\dagger 2} \rangle - \langle a^2 \rangle + 2\langle a^\dagger a \rangle - (\langle a^\dagger \rangle + \langle a \rangle)^2\}. \end{cases} \quad (31)$$

Similarly, with the employment of the bosonic operator definitions for the collective atomic operators, the quadrature variances of the atomic ensemble can be given as

$$\begin{cases} (\Delta q_b)^2 &= \frac{1}{2\tilde{\omega}_0} \{1 + \langle b^{\dagger 2} \rangle + \langle b^2 \rangle + 2\langle b^\dagger b \rangle - (\langle b^\dagger \rangle + \langle b \rangle)^2\}, \\ (\Delta p_b)^2 &= \frac{\tilde{\omega}_0}{2} \{1 - \langle b^{\dagger 2} \rangle - \langle b^2 \rangle + 2\langle b^\dagger b \rangle - (\langle b^\dagger \rangle + \langle b \rangle)^2\}. \end{cases} \quad (32)$$

It is well known that a bosonic mode would be squeezed when one of its quadrature variances is less than the uncertainty [60]. That is to say, the cavity field and atomic ensemble would be squeezed when the one value of $(\Delta q_{j=a,b})^2$ and $(\Delta p_{j=a,b})^2$ is less than 1/2 (uncertainty in coherent state). In the normal phase, the variances can be written by the linear combinations of the bosonic operators $\{d_1^\dagger, d_1, d_2^\dagger, d_2\}$ (see Appendix A). By taking the ground-state expectation value, we can obtain the expressions of the variances as Appendix B. In the super-radiant phase, we can apply the displacement transformation on bosonic modes, then quadrature variances of the cavity mode and atomic ensemble in the super-radiant phase can be given as

$$\begin{cases} (\Delta q_a)^2 &= (\Delta X_a)^2, \\ (\Delta q_b)^2 &= \tilde{\omega}_0/\omega_0(\Delta X_b)^2, \\ (\Delta p_a)^2 &= (\Delta P_a)^2, \\ (\Delta p_b)^2 &= \tilde{\omega}_0/\omega_0(\Delta P_b)^2. \end{cases} \quad (33)$$

The analytic solutions of these variances in the ground states, which are shown in Appendix B, are plotted in Figure 4 by using Equations (31) and (32). First of all, we consider the case for $f = 0$ in Figure 4a. In the normal phase, $(\Delta p_a)^2$ and $(\Delta p_b)^2$ are

coincident with each other, and it is the same for $(\Delta q_a)^2$ and $(\Delta q_b)^2$. Moreover, when χ approaches χ_c , the variances $(\Delta q_a)^2$ and $(\Delta q_b)^2$ increase, but there is a slight squeezing in the momentum variances. In the super-radiant phase, the position variances $(\Delta q_a)^2$ and $(\Delta q_b)^2$ reduce rapidly, while the momentum variances $(\Delta p_a)^2$ and $(\Delta p_b)^2$ increase slowly for the increase of the coupling strength. The best squeezing of the momentum variances occurs at the point for QPT ($\chi = 0.5$). The above squeezing results from that our system is a specific example of the Bogoliubov transformation with squeezing properties, which are the same as the ones in Refs. [58,61].

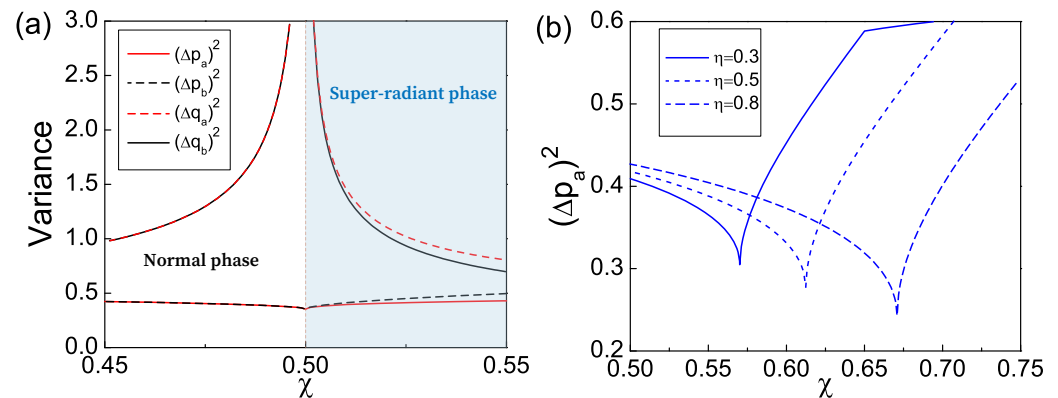


Figure 4. (a) The quadrature variances for cavity mode and atoms in the ground state of our system in the thermodynamic limit. (b) The momentum variances of cavity mode versus the coupling strength χ with the different force ratio η . The other parameters are same as Figure 2.

To explore the relation between the squeezed field and the external force ($f \neq 0$), it is necessary to simulate the critical values of QPT with different force ratios η . Here we only consider the momentum variance of cavity mode $(\Delta p_a)^2$ in Figure 4b. It shows, with the increase of the external force, the squeezing degree of cavity mode will be enhanced. The best squeezing degree occurs at the critical values of QPT, which are determined by the external force. Thus it is possible to detect the external force through the ground-state squeezing variances in the thermodynamic limit.

The smallest momentum variance of cavity mode versus the force ratio η with different χ are simulated in Figure 5. It illustrates the squeezing external force $f = \eta f_0$ can enhance the squeezing degree of cavity mode. Simultaneously, the sensitivity of the external force can also be improved by the squeezing degree of cavity mode, and the largest sensitivity for $\chi = \chi_c$ in Figure 5 is $\partial f / \partial (\Delta p_a)^2 = 1.54 f_0 / \omega_a$, while the one for $\chi = 0$ is zero. These phenomena indicate, without a driven field, it is impossible to achieve the precision measurement by using optomechanics, whereas the hybrid atom-optomechanical system can be employed to realize a precision measurement for squeezing properties. These results can be understood as follows. The QPT, caused by quantum fluctuation in the thermodynamic limit via the interaction between atomic ensemble and cavity mode [28], is irrelevant to the driven field. When the atomic ensemble is decoupled to the cavity mode ($\chi = 0$), our system will work in the normal phase as Figure 2 and behavior as a single optomechanics without driven field, no squeezing properties and output field can be employed to detect the external force. On the other hand, when the coupling strength χ is large enough, the quantum fluctuation will cause the super-radiant transition, then the squeezing properties can be measured and used to detect the external force. In other words, the quantum fluctuation in super-radiant phase ensures the hybrid atom-optomechanical system can realize the precision measurement without driven field. It is out of reach by using a single optomechanical cavity [10,23,24].

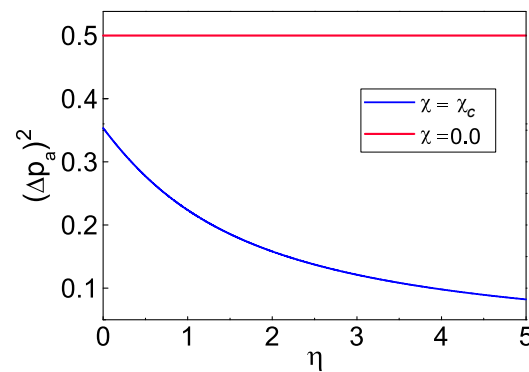


Figure 5. The smallest momentum variance of cavity mode versus the force ratio $\eta = f/f_0$ at the point of QPT by using Equations (31) and (32). All the rest parameters are the same as Figure 2.

5. Conclusions

In conclusion, we have studied and explored the relation between the super-radiant phase transition and external force in the hybrid optomechanical system. The special characters of the hybrid optomechanical cavity, e.g., force dependent quantum phase transition, can be fully controlled by the external force as the critical value of QPT can be modified by the external force. Specially, we illustrate that the squeezing properties of QPT can be employed to improve the sensitivity of the force measurement. We believe that our proposal provides a new way to realize the precise measurement with squeezing properties around QPT, which would show the great potential applications for the hybrid atom-optomechanical system.

Author Contributions: Conceptualization, J.-Q.Z.; formal analysis, data curation, L.L.; writing—review and editing, J.-Q.Z. and L.L. All authors have read and agreed to the published version of the manuscript.

Funding: This work is supported by the National Natural Science Foundation of China (Nos.91636220, 11835011, and 11847006), Key Research and Development Project of Guangdong Province (Grant No. 2020B030300001), Youth Support Plan Fund (No. 2017QNJH21) from Henan University of Technology and Cultivation Programme for Young Backbone Teachers in Henan University of Technology.

Institutional Review Board Statement: Not applicable.

Informed Consent Statement: Not applicable.

Data Availability Statement: Not applicable.

Conflicts of Interest: The authors declare no conflict of interest.

Appendix A. The Mode Transformation

Appendix A.1. Normal Phase

The set of bosons $\{a, b\}$ can be expressed in terms of bosons $\{d_1, d_2\}$ as

$$a^\dagger = \frac{1}{2} \left\{ \frac{\cos \theta_1}{\sqrt{\tilde{\omega}_a \lambda_-^N}} [(\tilde{\omega}_a + \lambda_-^N) d_1^\dagger + (\tilde{\omega}_a - \lambda_-^N) d_1] + \frac{\sin \theta_1}{\sqrt{\tilde{\omega}_a \lambda_+^N}} [(\tilde{\omega}_a + \lambda_+^N) d_2^\dagger + (\tilde{\omega}_a - \lambda_+^N) d_2] \right\}, \tag{A1}$$

$$a = \frac{1}{2} \left\{ \frac{\cos \theta_1}{\sqrt{\tilde{\omega}_a \lambda_-^N}} [(\tilde{\omega}_a + \lambda_-^N) d_1 + (\tilde{\omega}_a - \lambda_-^N) d_1^\dagger] + \frac{\sin \theta_1}{\sqrt{\tilde{\omega}_a \lambda_+^N}} [(\tilde{\omega}_a + \lambda_+^N) d_2 + (\tilde{\omega}_a - \lambda_+^N) d_2^\dagger] \right\}, \tag{A2}$$

$$b^\dagger = \frac{1}{2} \left\{ \frac{-\sin \theta_1}{\sqrt{\omega_0 \lambda_-^N}} [(\omega_0 + \lambda_-^N) d_1^\dagger + (\omega_0 - \lambda_-^N) d_1] + \frac{\cos \theta_1}{\sqrt{\omega_0 \lambda_+^N}} [(\omega_0 + \lambda_+^N) d_2^\dagger + (\omega_0 - \lambda_+^N) d_2] \right\}, \tag{A3}$$

$$b = \frac{1}{2} \left\{ \frac{-\sin \theta_1}{\sqrt{\omega_0 \lambda_-^N}} [(\omega_0 + \lambda_-^N) d_1 + (\omega_0 - \lambda_-^N) d_1^\dagger] + \frac{\cos \theta_1}{\sqrt{\omega_0 \lambda_+^N}} [(\omega_0 + \lambda_+^N) d_2 + (\omega_0 - \lambda_+^N) d_2^\dagger] \right\}, \tag{A4}$$

The angle θ_1 is the rotation angle of the coordinate system, which eliminates the interaction in the position representation.

Appendix A.2. Super-Radiant Phase

The analogous Bogoliubov transformations in the super-radiant phase are

$$A^\dagger = \frac{1}{2} \left\{ \frac{\cos \theta_2}{\sqrt{\tilde{\omega}_a \lambda_-^S}} [(\tilde{\omega}_a + \lambda_-^S) e_1^\dagger + (\tilde{\omega}_a - \lambda_-^S) e_1] + \frac{\sin \theta_2}{\sqrt{\tilde{\omega}_a \lambda_+^S}} [(\tilde{\omega}_a + \lambda_+^S) e_2^\dagger + (\tilde{\omega}_a - \lambda_+^S) e_2] \right\}, \tag{A5}$$

$$A = \frac{1}{2} \left\{ \frac{\cos \theta_2}{\sqrt{\tilde{\omega}_a \lambda_-^S}} [(\tilde{\omega}_a + \lambda_-^S) e_1 + (\tilde{\omega}_a - \lambda_-^S) e_1^\dagger] + \frac{\sin \theta_2}{\sqrt{\tilde{\omega}_a \lambda_+^S}} [(\tilde{\omega}_a + \lambda_+^S) e_2 + (\tilde{\omega}_a - \lambda_+^S) e_2^\dagger] \right\}, \tag{A6}$$

$$B^\dagger = \frac{1}{2} \left\{ \frac{-\sin \theta_2}{\sqrt{\tilde{\omega}_0 \lambda_-^S}} [(\tilde{\omega}_0 + \lambda_-^S) e_1^\dagger + (\tilde{\omega}_0 - \lambda_-^S) e_1] + \frac{\cos \theta_2}{\sqrt{\tilde{\omega}_0 \lambda_+^S}} [(\tilde{\omega}_0 + \lambda_+^S) e_2^\dagger + (\tilde{\omega}_0 - \lambda_+^S) e_2] \right\}, \tag{A7}$$

$$B = \frac{1}{2} \left\{ \frac{-\sin \theta_2}{\sqrt{\tilde{\omega}_0 \lambda_-^S}} [(\tilde{\omega}_0 + \lambda_-^S) e_1 + (\tilde{\omega}_0 - \lambda_-^S) e_1^\dagger] + \frac{\cos \theta_2}{\sqrt{\tilde{\omega}_0 \lambda_+^S}} [(\tilde{\omega}_0 + \lambda_+^S) e_2 + (\tilde{\omega}_0 - \lambda_+^S) e_2^\dagger] \right\}. \tag{A8}$$

Appendix B. Variance

In the thermodynamic limit, Bogoliubov transformations would be applied to derive exact expressions for the squeezing variances of the ground state. In the normal phase, we can rewritten Equations (31) and (32) as

$$(\Delta q_a)^2 = \frac{1}{2\tilde{\omega}_a} \left(1 + \frac{\lambda_+^N (\tilde{\omega}_a - \lambda_-^N) \cos^2 \theta_1 + \lambda_-^N (\tilde{\omega}_a - \lambda_+^N) \sin^2 \theta_1}{\lambda_-^N \lambda_+^N} \right), \tag{A9}$$

$$(\Delta p_a)^2 = \frac{\tilde{\omega}_a}{2} \left(1 + \frac{(\lambda_-^N - \tilde{\omega}_a) \cos^2 \theta_1 + (\lambda_+^N - \tilde{\omega}_a) \sin^2 \theta_1}{\tilde{\omega}_a} \right), \tag{A10}$$

$$(\Delta q_b)^2 = \frac{1}{2\omega_0} \left(1 + \frac{\lambda_+^N (\omega_0 - \lambda_-^N) \sin^2 \theta_1 + \lambda_-^N (\omega_0 - \lambda_+^N) \cos^2 \theta_1}{\lambda_-^N \lambda_+^N} \right), \tag{A11}$$

$$(\Delta p_b)^2 = \frac{\omega_0}{2} \left(1 + \frac{(\lambda_-^N - \omega_0) \sin^2 \theta_1 + (\lambda_+^N - \omega_0) \cos^2 \theta_1}{\omega_0} \right). \tag{A12}$$

In the super-radiant phase, we can rewrite Equation (32) as

$$(\Delta q_a)^2 = \frac{1}{2\tilde{\omega}_a} \left(1 + \frac{\lambda_+^S (\tilde{\omega}_a - \lambda_-^S) \cos^2 \theta_2 + \lambda_-^S (\tilde{\omega}_a - \lambda_+^S) \sin^2 \theta_2}{\lambda_-^S \lambda_+^S} \right), \tag{A13}$$

$$(\Delta p_a)^2 = \frac{\tilde{\omega}_a}{2} \left(1 + \frac{(\lambda_-^S - \tilde{\omega}_a) \cos^2 \theta_2 + (\lambda_+^S - \tilde{\omega}_a) \sin^2 \theta_2}{\tilde{\omega}_a} \right), \tag{A14}$$

$$(\Delta q_b)^2 = \frac{1}{2\omega_0} \left(1 + \frac{\lambda_+^S (\tilde{\omega}_0 - \lambda_-^S) \sin^2 \theta_2 + \lambda_-^S (\tilde{\omega}_0 - \lambda_+^S) \cos^2 \theta_2}{\lambda_-^S \lambda_+^S} \right), \tag{A15}$$

$$(\Delta p_b)^2 = \frac{\omega_0}{2} \left(1 + \frac{(\lambda_-^S - \tilde{\omega}_0) \sin^2 \theta_2 + (\lambda_+^S - \tilde{\omega}_0) \cos^2 \theta_2}{\tilde{\omega}_0} \right). \tag{A16}$$

These results are plotted in Figure 4.

References

1. Bose, S.; Jacobs, K.; Knight, P.L. Preparation of nonclassical states in cavities with a moving mirror. *Phys. Rev. A* **1997**, *56*, 4175. [[CrossRef](#)]
2. Vitali, D.; Gigan, S.; Ferreira, A.; Böhm, H.R.; Tombesi, P.; Guerreiro, A.; Vedral, V.; Zeilinger, A.; Aspelmeyer, M. Optomechanical entanglement between a movable mirror and a cavity field. *Phys. Rev. Lett.* **2007**, *98*, 030405. [[CrossRef](#)]
3. Sun, L.H.; Li, G.X.; Ficek, Z. First-order coherence versus entanglement in a nanomechanical cavity. *Phys. Rev. A* **2012**, *85*, 022327. [[CrossRef](#)]
4. Liao, J.Q.; Law, C.K. Parametric generation of quadrature squeezing of mirrors in cavity optomechanics. *Phys. Rev. A* **2011**, *83*, 033820. [[CrossRef](#)]
5. Han, Y.; Cheng, J.; Zhou, L. The quadrature squeezing of a mirror in cavity optomechanics coupled with atomic media. *Eur. Phys. J. D* **2013**, *67*, 20. [[CrossRef](#)]
6. Agarwal, G.S.; Huang, S.M. Electromagnetically induced transparency in mechanical effects of light. *Phys. Rev. A* **2010**, *81*, 041803. [[CrossRef](#)]
7. Huang, S.M.; Agarwal, G.S. Electromagnetically induced transparency from two-phonon processes in quadratically coupled membranes. *Phys. Rev. A* **2011**, *83*, 023823. [[CrossRef](#)]
8. Safavi-Naeini, A.H.; Alegre, T.P.M.; Chan, J.; Eichenfield, M.; Winger, M.; Lin, Q.; Hill, J.T.; Chang, D.E.; Painter, O. Electromagnetically induced transparency and slow light with optomechanics. *Nature* **2011**, *472*, 69. [[CrossRef](#)]
9. Weis, S.; Rivière, R.; Deléglise, S.; Gavartin, E.; Arcizet, O.; Schliesser, A.; Kippenberg, T.J. Optomechanically induced transparency. *Science* **2010**, *330*, 1520. [[CrossRef](#)]
10. Zhang, J.-Q.; Li, Y.; Feng, M.; Xu, Y. Precision measurement of electrical charge with optomechanically induced transparency. *Phys. Rev. A* **2012**, *86*, 053806. [[CrossRef](#)]
11. Lü, X.Y.; Jing, H.; Ma, J.Y.; Wu, Y. PT-symmetry-breaking chaos in optomechanics. *Phys. Rev. Lett.* **2015**, *114*, 253601. [[CrossRef](#)]
12. Bakemeier, L.; Alvermann, A.; Fehske, H. Route to chaos in optomechanics. *Phys. Rev. Lett.* **2015**, *114*, 013601. [[CrossRef](#)]
13. Agarwal, G.S.; Huang, S.M. Optomechanical systems as single-photon routers. *Phys. Rev. A* **2012**, *85*, 021801. [[CrossRef](#)]
14. Xiong, H.; Si, L.G.; Yang, X.X.; Wu, Y. Asymmetric optical transmission in an optomechanical array. *Appl. Phys. Lett.* **2015**, *107*, 091116. [[CrossRef](#)]
15. Gröblacher, S.; Hammerer, K.; Vanner, M.R.; Aspelmeyer, M. Observation of strong coupling between a micromechanical resonator and an optical cavity field. *Nature* **2009**, *460*, 724. [[CrossRef](#)]
16. Thompson, J.D.; Zwickl, B.M.; Jayich, A.M.; Marquardt, F.; Girvin, S.M.; Harris, J.G.E. Strong dispersive coupling of a high-finesse cavity to a micromechanical membrane. *Nature* **2008**, *452*, 72. [[CrossRef](#)]
17. Li, Y.; Wang, Y.D.; Xue, F.; Bruder, C. Quantum theory of transmission line resonator-assisted cooling of a micromechanical resonator. *Phys. Rev. B* **2008**, *78*, 134301. [[CrossRef](#)]
18. Wilson-Rae, I.; Zoller, P.; Imamoglu, A. Laser cooling of a nanomechanical resonator mode to its quantum ground state. *Phys. Rev. Lett.* **2004**, *92*, 075507. [[CrossRef](#)]
19. Wilson-Rae, I.; Nooshi, N.; Zwerger, W.; Kippenberg, T.J. Theory of ground state cooling of a mechanical oscillator using dynamical backaction. *Phys. Rev. Lett.* **2007**, *99*, 093901. [[CrossRef](#)]
20. Marquardt, F.; Chen, J.P.; Clerk, A.A.; Girvin, S.M. Quantum theory of cavity-assisted sideband cooling of mechanical motion. *Phys. Rev. Lett.* **2007**, *99*, 093902. [[CrossRef](#)]
21. Xia, K.; Evers, J. Ground State Cooling of a Nanomechanical Resonator in the Nonresolved Regime via Quantum Interference. *Phys. Rev. Lett.* **2009**, *103*, 227203. [[CrossRef](#)] [[PubMed](#)]
22. Li, L.C.; Luo, R.H.; Liu, L.J.; Zhang, S.; Zhang, J.Q. Double-passage ground-state cooling induced by quantum interference in the hybrid optomechanical system. *Sci. Rep.* **2018**, *8*, 14276. [[CrossRef](#)]
23. Schliesser, A.; Arcizet, O.; Rivière, R.; Anetsberger, G.; Kippenberg, T.J. Resolved-sideband cooling and position measurement of a micromechanical oscillator close to the Heisenberg uncertainty limit. *Nat. Phys.* **2009**, *5*, 509. [[CrossRef](#)]
24. He, Y. Sensitivity of optical mass sensor enhanced by optomechanical coupling. *Appl. Phys. Lett.* **2011**, *106*, 121905. [[CrossRef](#)]
25. Andreev, A.V.; Emel'yanov, V.I.; Il'Inskii, Y.A. *Cooperative Effects in Optics: Superradiance and Phase Transitions*; Institute of Physics Pub: Bristol, UK, 1993.
26. Benedict, M.G. *Super-Radiance: Multiatomic Coherent Emission*; CRC Press: Los Angeles, CA, USA, 2018.
27. Rehler, N.E.; Eberly, J.H. Superradiance. *Phys. Rev. A* **1971**, *3*, 1735. [[CrossRef](#)]
28. Hepp, K.; Lieb, E.H. On the super-radiant phase transition for molecules in a quantized radiation field: The Dicke maser model. *Ann. Phys.* **1973**, *76*, 360. [[CrossRef](#)]
29. Wang, Y.K.; Hioe, F.T. Phase transition in the Dicke model of superradiance. *Phys. Rev. A* **1973**, *7*, 831. [[CrossRef](#)]
30. Lewenkopf, C.H.; Nemes, M.C.; Marvulle, V.; Pato, M.P.; Wreszinski, W.F. Level statistics transitions in the spin-boson model. *Phys. Lett. A* **1991**, *155*, 113. [[CrossRef](#)]
31. Furuya, K.; Nemes, M.C.; Pellegrino, G.Q. Quantum dynamical manifestation of chaotic behavior in the process of entanglement. *Phys. Rev. Lett.* **1998**, *80*, 5524. [[CrossRef](#)]

32. Angelo, R.M.; Furuya, K.; Nemes, M.C.; Pellegrino, G.Q. Recoherence in the entanglement dynamics and classical orbits in the N-atom Jaynes-Cummings model. *Phys. Rev. A* **2001**, *64*, 043801. [[CrossRef](#)]
33. Emary, C.; Brandes, T. Quantum chaos triggered by precursors of a quantum phase transition: The Dicke model. *Phys. Rev. Lett.* **2003**, *90*, 044101. [[CrossRef](#)] [[PubMed](#)]
34. Hou, X.W.; Hu, B. Decoherence, entanglement, and chaos in the Dicke model. *Phys. Rev. A* **2004**, *69*, 042110. [[CrossRef](#)]
35. Lambert, N.; Emary, C.; Brandes, T. Entanglement and the phase transition in single-mode superradiance. *Phys. Rev. Lett.* **2004**, *92*, 073602. [[CrossRef](#)] [[PubMed](#)]
36. Vidal, J.; Dusuel, S. Finite-size scaling exponents in the Dicke model. *Europhys. Lett.* **2006**, *74*, 817. [[CrossRef](#)]
37. Liu, T.; Zhang, Y.Y.; Chen, Q.H.; Wang, K.L. Large-N scaling behavior of the ground-state energy, fidelity, and the order parameter in the Dicke model. *Phys. Rev. A* **2009**, *80*, 023810. [[CrossRef](#)]
38. Dimer, F.; Estienne, B.; Parkins, A.S.; Carmichael, H.J. Proposed realization of the Dicke-model quantum phase transition in an optical cavity QED system. *Phys. Rev. A* **2007**, *75*, 013804. [[CrossRef](#)]
39. Chen, G.; Chen, Z.D.; Liang, J.Q. Simulation of the super-radiant quantum phase transition in the superconducting charge qubits inside a cavity. *Phys. Rev. A* **2007**, *76*, 055803. [[CrossRef](#)]
40. Boller, K.J.; Imamoglu, A.; Harris, S.E. Observation of electromagnetically induced transparency. *Phys. Rev. Lett.* **1991**, *66*, 2593. [[CrossRef](#)]
41. Teufel, J.D.; Donner, T.; Li, D.; Harlow, J.W.; Allman, M.S.; Cicak, K.; Sirois, A.J.; Whittaker, J.D.; Lehnert, K.W.; Simmonds, R.W. Sideband cooling of micromechanical motion to the quantum ground state. *Nature* **2011**, *475*, 359. [[CrossRef](#)]
42. Barzanjeh, S.; Abdi, M.; Milburn, G.J.; Tombesi, P.; Vitali, D. Reversible optical-to-microwave quantum interface. *Phys. Rev. Lett.* **2012**, *109*, 130503. [[CrossRef](#)]
43. Pflanzner, A.C.; Romero-Isart, O.; Cirac, J.I. Optomechanics assisted by a qubit: From dissipative state preparation to many-partite systems. *Phys. Rev. A* **2013**, *88*, 033804. [[CrossRef](#)]
44. Ian, H.; Gong, Z.R.; Liu, Y.X.; Sun, C.P.; Nori, F. Cavity optomechanical coupling assisted by an atomic gas. *Phys. Rev. A* **2008**, *78*, 013824. [[CrossRef](#)]
45. Genes, C.; Ritsch, H.; Drewsen, M.; Dantan, A. Atom-membrane cooling and entanglement using cavity electromagnetically induced transparency. *Phys. Rev. A* **2011**, *84*, 051801. [[CrossRef](#)]
46. Li, L.C.; Hu, X.M.; Rao, S.; Xu, J. Atom-mirror entanglement via cavity dissipation. *Phys. Rev. A* **2015**, *91*, 052320. [[CrossRef](#)]
47. Tan, H.T.; Sun, L.H. Hybrid Einstein-Podolsky-Rosen steering in an atom-optomechanical system. *Phys. Rev. A* **2015**, *92*, 063812. [[CrossRef](#)]
48. Zhang, S.; Zhang, J.Q.; Zhang, J.; Wu, C.W.; Wu, W.; Chen, P.X. Ground state cooling of an optomechanical resonator assisted by a Λ -type atom. *Opt. Express* **2014**, *22*, 28118. [[CrossRef](#)] [[PubMed](#)]
49. Vogell, B.; Stannigel, K.; Zoller, P.; Hammerer, K.; Rakher, M.T.; Korppi, M.; Jöckel, A.; Treutlein, P. Cavity-enhanced long-distance coupling of an atomic ensemble to a micromechanical membrane. *Phys. Rev. A* **2013**, *87*, 023816. [[CrossRef](#)]
50. Shi, X.F.; Bariani, F.; Kennedy, T.A.B. Entanglement of neutral-atom chains by spin-exchange Rydberg interaction. *Phys. Rev. A* **2014**, *90*, 062327. [[CrossRef](#)]
51. Jäger, S.B.; Cooper, J.; Holland, M.J.; Morigi, G. Nonequilibrium Quantum Phase Transition in a Hybrid Atom-Optomechanical System. *Phys. Rev. Lett.* **2018**, *120*, 063605. [[CrossRef](#)]
52. Jäger, S.B.; Cooper, J.; Holland, M.J.; Morigi, G. Dynamical Phase Transitions to Optomechanical Superradiance. *Phys. Rev. Lett.* **2019**, *123*, 053601. [[CrossRef](#)]
53. Wang, Z.; Lian, J.; Liang, J.Q.; Yu, Y.; Liu, W.M. Collapse of the superradiant phase and multiple quantum phase transitions for Bose-Einstein condensates in an optomechanical cavity. *Phys. Rev. A* **2016**, *93*, 033630. [[CrossRef](#)]
54. Santos, J.P.; Semiao, F.L.; Furuya, K. Probing the quantum phase transition in the Dicke model through mechanical vibrations. *Phys. Rev. A* **2010**, *82*, 063801. [[CrossRef](#)]
55. Wang, Y.; Liu, B.; Lian, J.; Liang, J. A scheme for detecting the atom-field coupling constant in the Dicke superradiation regime using hybrid cavity optomechanical system. *Phys. Rev. A* **2016**, *93*, 033630. [[CrossRef](#)]
56. Aggarwal, N.; Mahajana, S.; Bhattacharjee, A.B. Optomechanical effect on the Dicke quantum phase transition and quasi-particle damping in a Bose-Einstein condensate: A new tool to measure weak force. *J. Mod. Opt.* **2013**, *60*, 1263. [[CrossRef](#)]
57. Wu, Z.; Luo, R.H.; Zhang, J.Q.; Wang, Y.H.; Yang, W.; Feng, M. Force-induced transparency and conversion between slow and fast light in optomechanics. *Phys. Rev. A* **2017**, *96*, 033832. [[CrossRef](#)]
58. Emary, C.; Brandes, T. Chaos and the quantum phase transition in the Dicke model. *Phys. Rev. E* **2003**, *67*, 066203. [[CrossRef](#)] [[PubMed](#)]
59. Sachdev, S. *Quantum Phase Transitions. Handbook of Magnetism and Advanced Magnetic Materials*; John Wiley Sons Inc.: New York, NY, USA, 2007.
60. Glauber, R. Coherent and incoherent states of the radiation field. *Phys. Rev. Lett.* **1963**, *131*, 2766. [[CrossRef](#)]
61. Bishop, R.F.; Vourdas, A. Generalised coherent states and Bogoliubov transformations. *J. Phys. A* **1986**, *19*, 2525. [[CrossRef](#)]